MODELING, SIMULATION AND IMPLEMENTATION OF LOW POWER PHOTOVOLTAIC ENERGY CONVERSION SYSTEM

R. Sudharshan Kaarthik
Nayan Kumar Dalei
R. Vigneshwaran
Rabinarayan Das

Department of Electrical Engineering,
National Institute of Technology Rourkela,
Rourkela – 769008, India.

Modeling, Simulation and Implementation of Low Power Photovoltaic Energy Conversion System

Project Report Submitted in partial fulfillment of the requirements for the degree of

Bachelor of Technology

in

Electrical Engineering

by

R. Sudharshan Kaarthik (10602028)
Nayan Kumar Dalei (10602033)
R. Vigneshwaran (10602066)
Rabinarayan Das (10502002)

National Institute of Technology Rourkela,
Rourkela – 769008, India.

May 2010

Department of Electrical Engineering
National Institute of Technology Rourkela,
Rourkela – 769008, India. www.nitrkl.ac.in

B.Chitti Babu
Assistant Professor

May 13, 2010

CERTIFICATE

This is to certify that the project entitled *Modeling, Simulation and Implementation of Low Power Photovoltaic Energy Conversion System* submitted by Mr. *R. Sudharshan Kaarthik* (Roll No. 1602028), Mr. *Nayan Kumar Dalei* (Roll. No. 10602033), Mr. *R. Vigneshwaran* (10602066) and Mr. *Rabinarayan Das* (Roll No. 10502002) in partial fulfillment of the requirements for the award of Bachelor of Technology Degree in Electrical Engineering at NIT Rourkela is an authentic work carried out by them under my supervision and guidance.

B. Chitti Babu

ACKNOWLEDGEMENT

We would like to thank NIT Rourkela for giving us the opportunity to use their resources and work in such a challenging environment. First and foremost we take this opportunity to express our deepest sense of gratitude to our guide *Prof. B. Chitti Babu* for his able guidance during our project work. This project would not have been possible without his help and the valuable time that he has given us amidst his busy schedule. We would also like to extend our gratitude to our friends and senior students of this department who have always encouraged and supported in doing our work. Last but not the least we would like to thank all the staff members of Department of Electrical Engineering who have been very cooperative with us.

R. Sudharshan Kaarthik
Nayan Kumar Dalei
R. Vigneshwaran
Rabinarayan Das

TABLE OF CONTENTS

LIST OF FIGURES

ABSTRACT

Remote areas in India are still not connected to the power grid. But they have mobile network connectivity. The people face problems in charging their cell phones. They are forced to travel a long distances to get access to electrical outlets. This project focuses on providing a Photovoltaic System which could charge a cell phone battery. The developed system provides a solution to this problem. The system comprises of PV array, Maximum Power Point Tracker, Buck Converter and Charging Circuit. The system is modeled and simulated in Matlab-Simulink Environment. Hardware for the system is also implemented. We find proper synchronism between the results.

CHAPTER 1

INTRODUCTION

The use of new efficient photovoltaic solar cells (PVSCs) has emerged as an alternative measure of renewable green power, energy conservation and demand-side management. Owing to their high initial cost, PVSCs have not yet been fully an attractive alternative for electricity users who are able to buy cheaper electrical power from the utility grid. However, they can be used extensively for water pumping and air conditioning in remote and isolated areas, where utility power is not available or is too expensive to transport [1].

MOTIVATION

In India there are about 300 clear sunny days in a year and solar energy is available in most parts of the country, including the rural areas. But still we have miles to cover before solar power is effectively utilized to replace the fossil fuels and become a cheap and effective solution for domestic and commercial applications. With the growing demand for renewable sources of energy, the manufacturing of solar cells and photovoltaic arrays has advanced dramatically in recent years. Its efficient usage has led to increasing role of photovoltaic technology as scalable and robust means of harnessing renewable energy.

WORK SUMMARY

A photovoltaic energy conversion system for converting solar power into useable DC at 5V to 15V for charging batteries of low power devices like mobile phones has been proposed and implemented. The energy obtained from the photovoltaic module is unregulated. But for charging Lithium ion batteries, we require approximately 4.5V steady DC supply. The 18V unregulated DC obtained from the PV module is stepped down to 9V by DC-DC buck converter. Fig.1 shows the complete structure of PV energy conversion system, which comprises PV array with DC-DC buck converter.

The inductor design of the buck converter circuit is discussed in detail, which is a significant part in designing of the converter. For efficient usage of photovoltaic energy conversion system, it is essential to design a maximum power point tracking (MPPT) system. The concept of MPPT is to automatically vary a PV array's operating point so as to get maximum power [2]. This is necessary because the PV cell has a very low conversion efficiency and to reduce the cost of the overall system. The power delivered by array increases to maximum as the current drawn rises and after a particular value, the voltage falls suddenly making the power drop to zero. A boost converter is not preferred here because it cannot track maximum power point at low radiation levels, as this point is located in the non-operating region.

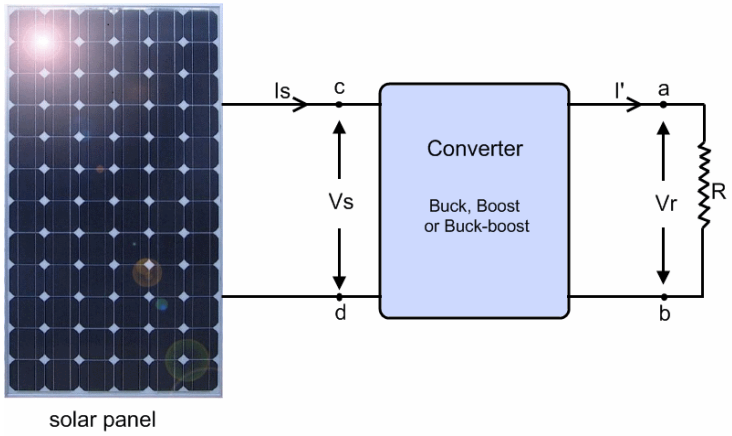

Fig. 1 - Complete Photovoltaic Energy Conversion System

REPORT ORGANIZATION

Renewable energy utilization in Indian scenario is presented in Chapter 2 along with the prospects of the photovoltaic energy. Characteristics of Photovoltaic cells are discussed in Chapter 3. Chapter 4 is about Maximum Power Point tracking and choice of MPP tracker. Chapter 5 elaborates on Buck converter operation. Chapter 6 discusses the practical implementation of the circuit. Chapter 7 is dedicated to results and discussion of the work done. Finally, Chapter 8 describes the concluding remarks and future work.

Simulation of the whole system has been carried out using Matlab-Simulink environment via the graphical user interface. The hardware implementation of the system is also made and we find proper correlation between the two.

CHAPTER 2

RENEWABLE ENERGY

In recent years, there is a substantial increase of energy consumption in India. This fast rate of energy consumption is influenced by the population growth and economic development in India. In the last four decades the commercial energy consumption in India has grown by about 700 percent. This has lead to the per capita consumption in India to be in region of 400 KWH per annum. Driven by the rise in population, ever expanding economy and an ultimate quest for improved quality of life, energy usage in India is expected to grow in an exponential rate.

Compared to the other developing countries the per capita energy consumption in India is still very low even though there is an overall increase in energy demand every year. Today, India is one of the potential competitors for the effective usage of renewable energy. India is the world's largest producer of wind power after Denmark, Germany, Spain and the USA. India has a significant potential for generation of power from renewable energy sources - Small hydro power, wind energy, bio-mass and solar energy.

RENEWABLE ENERGY SCENARIO IN INDIA

Renewable Energy in India is a sector that is still undeveloped. India was probably the first country in the world to set up a separate ministry of non-conventional energy resources in early 1980s. However the results have been very mixed and in recent years it has lagged far behind other developed nations in using renewable energy (RE). RE contribution to energy sector is less than 1% of India's total energy needs.

India is one of the largest and fastest growing economies in the world with an expansive populace of above 1.1 billion people. There is a very high demand for energy, which is currently satisfied mainly by coal, foreign oil and petroleum, which apart from being a non-renewable, and

therefore non-permanent solution to the energy crisis, it is also detrimental to the environment. The price of crude oil has risen sharply over the last few years, and there are no signs of a change in this trend [3]. Thus, it is imperative that India obtains energy security without affecting the booming economy, which would mean that alternative energy sources must be developed. This would mean that the country must switch from the non-renewable energy (crude oil and coal) to renewable energy. Figure 2 gives an account of installed power capacity of various power generation systems.

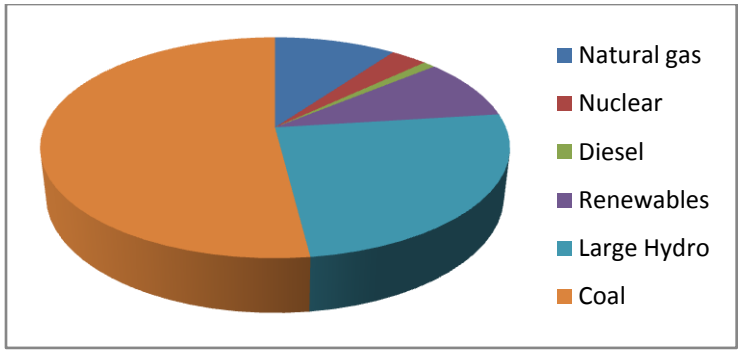

Fig. 2 - Percentage of installed Power capacity in India

India is determined to become one of the world's leading clean energy producers. The Government of India has already made several provisions, and established many agencies that will help it achieve its goal. Renewable Energy, excluding large hydro projects already accounts for 9% of the total installed energy capacity, equivalent to 12,610 MW. In combination with large hydro, the capacity is more than 34%, i.e. 48,643MW, in a total installed capacity of 1,44,980 MW. Refer figure 3.

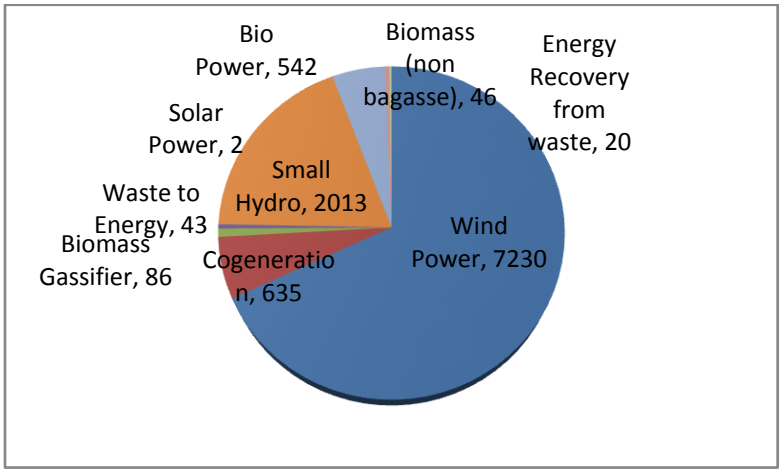

Fig. 3 - Renewable energy generation in India

SOLAR ENERGY IN INDIA

Solar power, a clean renewable resource with zero emission, has got tremendous potential of energy which can be harnessed using a variety of devices. With recent developments, solar energy systems are easily available for industrial and domestic use with the added advantage of minimum maintenance. Solar energy could be made financially viable with government tax incentives and rebates. An exclusive solar generation system of capacity of 250KWh per month would cost around Rs. 5 lakhs, with present pricing and taxes (2010). Most of the developed countries are switching over to solar energy as one of the prime renewable energy source. The current architectural designs make provision for photovoltaic cells and necessary circuitry while making building plans.

India is a country near the equator – which means that given its geographical location, it is subject to a large amount of solar irradiation throughout the year. India is also, according to area, the seventh largest country in the world. Combining the two points together, it is not difficult to gauge that solar energy in India is a vast and plentiful resource. Much of the country does not have access to electrical grid; one of the first applications of solar power has been for water pumping; to begin replacing India's four to five million diesel powered water pumps, each consuming about 3.5 kilowatts, and off-grid lighting. Some large projects have been proposed, and a 35,000 km^2 area of the Thar Desert has been set aside for solar power projects, sufficient to generate 700 to 2,100 Giga Watts.

About 7.7 lakhs solar lanterns, 5.1 lakhs solar home lighting systems, 82,500 solar street lighting systems, 7,247 solar water pumping systems, stand-alone and grid connected solar photovoltaic (SPV) power plants of about 10 MW peak aggregate capacity, about 3.12 million square meter solar water heater collector area and 6.57 lakhs solar cookers have been distributed/installed in the country, as on 30.11.2009, under the solar energy programs. The present cost of electricity generation from solar thermal and solar photovoltaic energy systems is Rs. 13.45 and Rs. 18.44 per unit, respectively as fixed by Central Electricity Regulatory Commission.

CHAPTER 3

PV CELL AND MODELING

I-V CHARACTERISTICS OF A PHOTOVOLTAIC MODULE

The performance characteristics of a photovoltaic module depend on its basic materials, manufacturing technology and operating conditions.

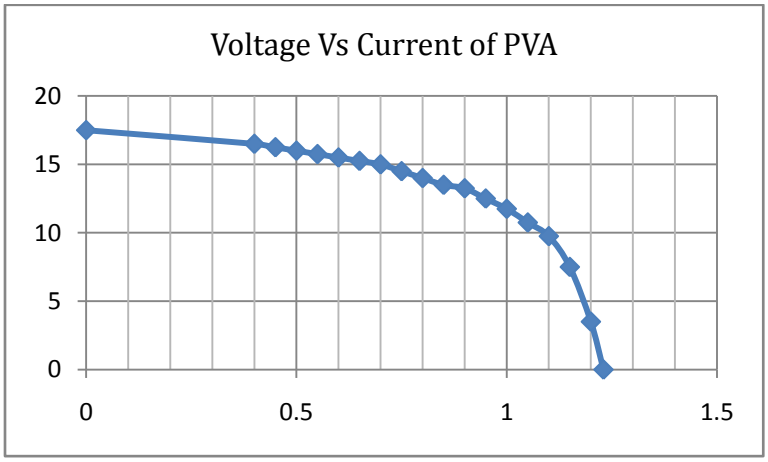

Fig. 4 - PVA Characteristics V (Y axis) Vs I (X axis)

Three points in these curves are of particular interest:

1. Short circuit point, where the voltage over the module is zero and the current is at its maximum (short circuit current I_{sc}).

2. Maximum power point or MPP, where the product of current and voltage has its maximum (defined by $I_{mpp}.V_{mpp}$).

3. Open circuit point, where the current is zero and the voltage has its maximum (open circuit voltage V_{oc}).

The measurements taken for obtaining an *I-V* curve is done by controlling the load current. At open circuit, when no load current is generated, a first characteristic value can be measured: the open circuit voltage V_{oc}. Increasing the load fed by the photovoltaic module leads to a decreasing voltage *V* with an increasing current *I*. In other words, by increasing the load current from zero to its maximum value, the operating point moves from the open circuit voltage at zero current to the short circuit current I_{sc} at zero voltage. The series of all measured pairs (*V*, *I*) yields the characteristic *I-V* curve of the module.

From the characteristic curve of the module, it is clear that the open circuit voltage of the photovoltaic module, the point of intersection of the curve with the horizontal axis, varies little with solar radiation changes. It is inversely proportional to temperature, i.e., a rise in temperature produces a decrease in voltage. Short circuit current, the point of intersection of the curve with the vertical axis, is directly proportional to solar radiation and is relatively steady with temperature variations. Actually, the photovoltaic module acts like a constant current source for most parts of its *I-V* curve [4].

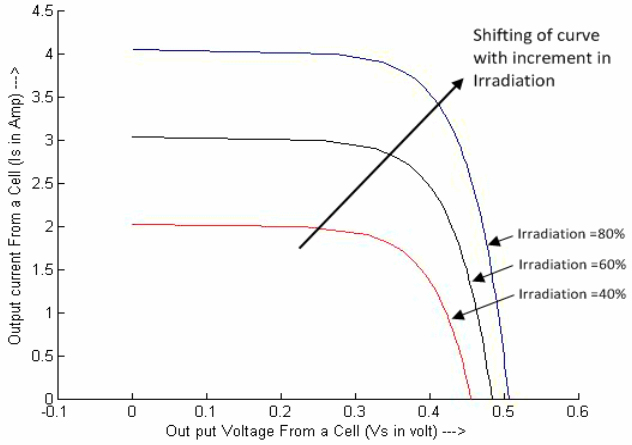

Fig 5. – Voltage Vs Current characteristics of PVA with Variation of Insolation

As demonstrated in Fig. 5, an increase in solar radiation causes the output current to increase and the horizontal part of the curve moves upward. An increase in cell temperature causes the voltage to move leftward, while decreasing temperature produces the opposite effect. Thus, the *I-V* curves display how a photovoltaic module responds to all possible loads under different solar radiation and cell temperature conditions.

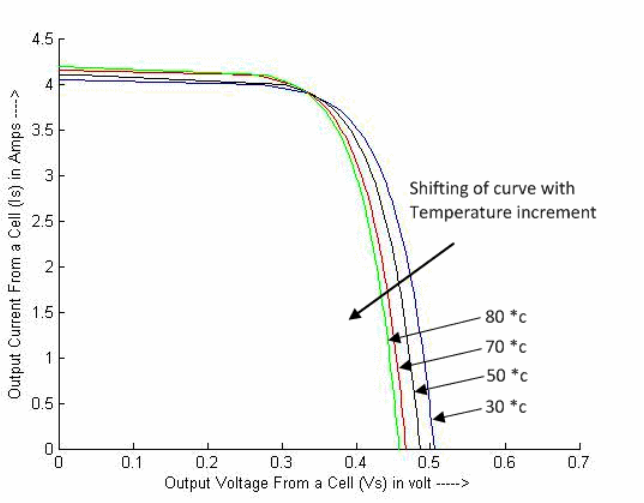

Fig. 6 – Characteristics of PVA incorporating effect of Temperature

The operating point of a photovoltaic module will move by varying solar radiation, cell temperature, and load values. For a given solar radiation and operating temperature, the output power depends on the value of the load current. As the load increases, the operating point moves along the curve towards the right. So, only one load value produces a maximum power. The maximum power points the line which is positioned at the knees of the *I-V* curves, has a nearly constant output voltage at varying solar radiation conditions. When the temperature varies, the maximum power points are generated in such a manner that the output current stays approximately constant.

The fill factor (FF) of a photovoltaic generator is defined as the ratio of output power at MPP to the power computed by multiplying V_{oc} by I_{sc}. It determines the shape of the photovoltaic generator characteristics. The factors which affect the fill factor are the series and shunt resistances of the photovoltaic generator. A good fill factor is between 0.6-0.8 [5]. As the photovoltaic generator degrades with age, its series resistance tends to increase resulting in a lower fill factor.

During the design of a PVA powered system, a simulation must be performed for system analysis and parameter settings. Therefore an efficient and user-friendly simulation model of the PVAs is always needed. The PVA model proposed in [6] is a circuit based model to be used with Simulink. The proposed model was simulated with various types of loads for performance checking.

PV arrays are built up with combined series/parallel combinations of PV solar cells, which are usually represented by a simplified equivalent circuit model such as the one given in Fig. 7 or by eq. (3.1)

$$V_c = \frac{AkT_c}{e}\ ln\left\{\frac{I_{ph}+I_0-I_c}{I_0}\right\} - R_s I_c \qquad (3.1)$$

The PV cell output voltage is a function of the photocurrent which is mainly determined by the load current and the solar radiation level during the operation where the symbols are defined as follows:

e : electron charge (1.602×10^{-19} ℃)
k : Boltzmann constant (1.38×10^{-23} J/K)
I_c : Cell output current, A
I_{ph} : Photocurrent - a function of irradiation level and junction temperature
I_0 : Reverse saturation current of diode (0.0002 A)
R_s : Series resistance of cell (0.001 Ω)
T_c : Reference cell operating temperature (20 °C)
V_c : Cell output voltage, V

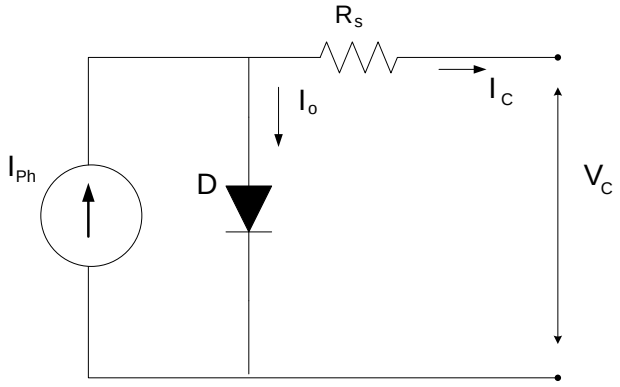

Fig. 7 - Simplified equivalent circuit of PV Array

Both k and T_c should have the same temperature unit, i.e. ℃ or Kelvin. The curve fitting factor A is used to adjust the *I-V* characteristics of the cell obtained from eq. (3.1) to the actual characteristics obtained by testing. The equation also gives the voltage of a single solar cell which is then multiplied by the number of the cells connected in series to calculate the full array voltage. Since the array current is the sum of the currents flowing through the cells in parallel branches, the cell

current I_C is obtained by dividing the array current by the number of cells connected in parallel before being used in eq. (3.1), which is only valid for a certain operating temperature T_c with its corresponding solar irradiation level S_c. If the temperature and solar irradiation level changes, the voltage and current output of the PV array will follow this change. Hence, the effects of the changes in temperature and solar irradiation levels should be included in the final PV array model.

TEMPERATURE AND IRRADIATION CORRECTION FACTORS

For a known temperature and a known solar irradiation level, a model is obtained and then this model is modified to handle different cases of temperatures and irradiation levels. Eq. (3.1) is the benchmark model for the known operating temperature T_c and known solar irradiation level S_c as given in the specification. When the ambient temperature and irradiation level change, the cell operating temperature also changes, resulting in a new output voltage and a new photocurrent value. The solar cell operating temperature varies as a function of solar irradiation level and ambient temperature. The ambient temperature T_a affects the cell output voltage and cell photocurrent. These effects are represented in the model by the temperature coefficients C_{TV} and C_{TI} for cell output voltage and cell photocurrent, respectively, as

$$C_{TV} = 1 + \beta_T (T_a - T_x) \tag{3.2}$$

$$C_{TI} = 1 + \frac{\gamma_T}{S_C} (T_a - T_x) \tag{3.3}$$

where, β_T = 0.004 and γ_T = 0.06 for the cell used and T_a=20°C is the ambient temperature during the cell testing. This is used to obtain the modified model of the cell for another ambient temperature T_x. Even if the ambient temperature does not change significantly during the daytime, the solar irradiation level changes depending on the sunlight and clouds.

A change in solar irradiation level causes a change in the cell photocurrent and operating temperature, which in turn affects the cell output voltage. If the solar irradiation level increases from S_{x1} to S_{x2}, the cell operating temperature and the photocurrent will increase from T_{x1} to T_{x2} and from I_{phl} to I_{ph2}, respectively. Thus the change in the operating temperature and the photocurrent due to variation in the solar irradiation level can be expressed with the help of two constants, C_{SV} and C_{SI}, which are the correction factors for changes in cell output voltage V_C and photocurrent I_{ph}, respectively.

$$C_{SV} = 1 + \beta_T \alpha_S (S_x - S_c) \tag{3.4}$$

$$C_{SI} = \frac{1}{S_C} (S_x - S_c) \tag{3.5}$$

where, S_c is the benchmark reference solar irradiation level during the cell testing. S_x is the new level of the solar irradiation. The temperature change ΔT_C occurs due to the change in the solar irradiation level which is obtained using

$$\Delta T_c = \alpha_S (S_x - S_c) \tag{3.6}$$

The constant α_S represents the slope of the change in the cell operating temperature due to a change in the solar irradiation level and is equal to 0.2 for the PVA used. Using correction factors C_{TV}, C_{TI}, C_{SV} and C_{SI}, the new values of the cell output voltage V_{Cx} and photocurrent I_{phx} are obtained for the new temperature T_x and solar irradiation S_x.

$$V_{CX} = C_{SV}\ C_{TV}\ V_C \tag{3.7}$$

$$I_{phx} = C_{SI}\ C_{TI}\ I_{ph} \tag{3.8}$$

V_C and I_{ph} are the benchmark reference cell output voltage and reference cell photocurrent, respectively. The Current versus voltage graph and the power versus voltage graphs for the simulated model and the actual solar panel are attached in the discussion section.

CHAPTER 4

MAXIMUM POWER POINT TRACKING

The power output from the solar panel is a function of insolation level and temperature. But for a given operating condition, we have a curve which gives the voltage level maintained by the panel for a particular value of current. This plot is known as the characteristics of the cell. From the characteristics plot, we will be able to derive the power output with respect to the output current. From [7] we adopt the method to find the current which has to be extracted so as to fix the operating point of the cell at its maximum power.

The operating point of any source sink mechanism is the intersection point of load line with the source characteristic plot [8]. What we attempt here to do is change the load angle theta (θ) to intersect the characteristics at maximum power point. The principle is described below.

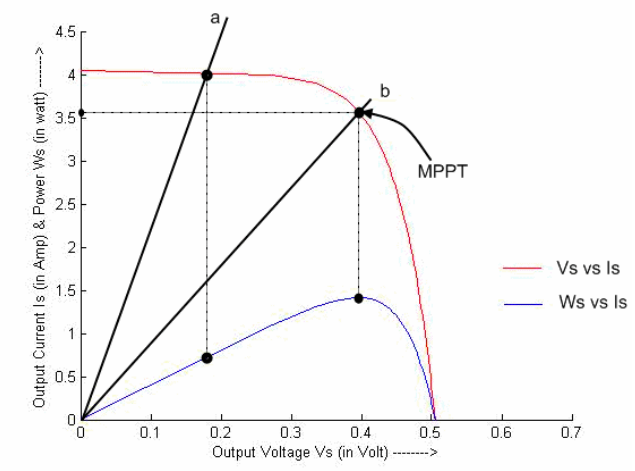

Fig. 8 – Operating point of PVA

Photovoltaic modules have a very low conversion efficiency of around 15% for the manufactured ones. Besides, due to the temperature, radiation and load variations, this efficiency can be highly reduced. In fact, the efficiency of any semiconductor device drops steeply with the temperature. In order to ensure that the photovoltaic modules always act supplying the maximum power as possible and dictated by ambient operating conditions, a specific circuit known as Maximum Power Point Tracker (MPPT) is employed.

In most common applications, the MPPT is a DC-DC converter controlled through a strategy that allows imposing the photovoltaic module operation point on the Maximum Power Point (MPP) or close to it. On the literature, many studies describing techniques to improve MPP algorithms were published [9], [10], permitting more velocity and precision of tracking. On the other hand, there is no a theory to guide the designer to choose, among the DC-DC converters family, the best one to operate as MPPT, thus, in most cases, the designers are tempted to use the simplest DC-DC converters – namely buck converter or boost converter.

CONVERTER CHOICE FOR MPPT

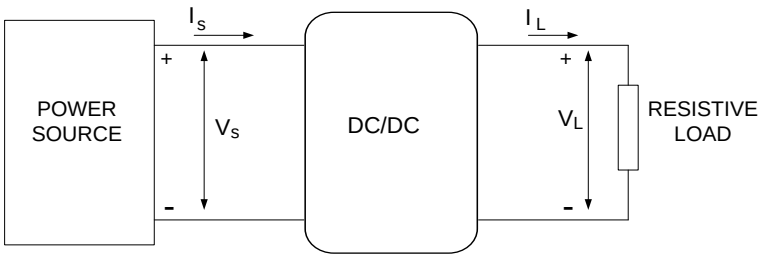

Fig. 9 – Converter acting as a Maximum Power Point Tracker

The load voltage can be obtained in terms of load current by the relation

$$V_{load} = I_{load} \times R_{load} \tag{4.1}$$

where V_{load} is the load voltage, I_{load} is the load current and R_{load} is the load resistance. We shall assume the operation of a buck converter and proceed in the analysis.

$$V_{load} = D \times V_{module} \tag{4.2}$$

The average input power to the DC-DC converter equals the average output power thereby, we get a relation

$$I_{load} = \frac{I_{module}}{D} \tag{4.3}$$

Combining the above two equations, we write

$$\frac{V_{module}}{I_{module}} = \frac{R_{load}}{D^2} \tag{4.4}$$

D here represents the voltage conversion ratio of the buck converter. So, when seen from the source side, the effective resistance will be $\frac{R_{load}}{D^2}$. This is a function of D, which we can control to fix the operating point near the MPP. We have to note that the range of D is zero to one.

$$D \in [0,1] \tag{4.5}$$

The load line is a straight line through the origin. So we can express the angle of inclination as

$$\theta\ (D, R_{load}) = \tan^{-1}\left(\frac{D^2}{R_{load}}\right) \tag{4.6}$$

Hence the range of angle is also fixed from zero to arctan(1/R)

$$\theta\ (D, R_{load}) \in \left[0, \tan^{-1}\frac{1}{R_{load}}\right] \tag{4.7}$$

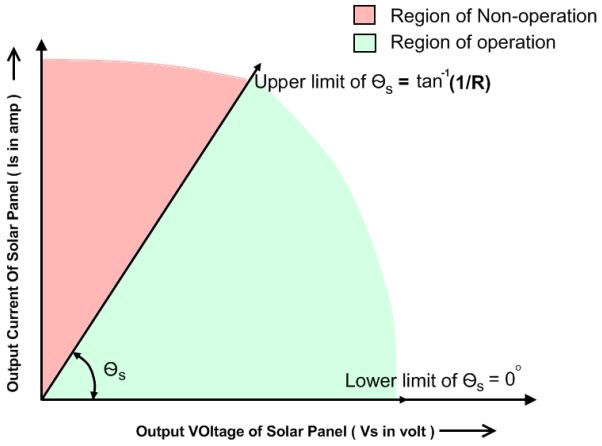

Fig. 10 – Region of operation of Buck Converter

The above results allow an important verification. When a Buck converter is applied as MPPT, the maximum power point will be tracked just if it is localized into the operation region. In any other case, the load and generation curves intersection will determinate the operation point. Still, it is important to notice that the load connected to the module imposes the upper angle limit, thus, when this load is changed, the system can operate at non-operational region, i.e., out of the MPP. Applying the same procedure to the others DC-DC converters, similar results are obtained. Depending on the static transfer characteristic of each DC-DC converter, the resistance $R_{load}(D,R)$ is characterized by a different equation. Table-1 summarizes these equations for DC-DC Buck, Boost, Buck-Boost, Cuk, Sepic and Zeta converters.

Table 1 - Conversion Factor and Range of Operation of Converters

DC-DC Converter	$\boldsymbol{R_e(D, R_{load})}$	**Range $\boldsymbol{\theta}$**
Buck Converter	$\frac{R_{load}}{D^2}$	$0° \leq \theta \leq \tan^{-1}\left(\frac{1}{R_{load}}\right)$
Boost Converter	$(1-D)^2 R_{load}$	$\tan^{-1}\left(\frac{1}{R_{load}}\right) \leq \theta \leq 90°$
Buck-Boost Converter / Cuk converter	$\left(\frac{1-D}{D}\right)^2 R_{load}$	$0° \leq \theta \leq 90°$

As the MPP is always requested, and this point can be found in any position on I-V curve, depending on temperature and radiation levels, the natural DC-DC converters to be applied as MPP Trackers are Buck-Boost, Cuk, Sepic or Zeta, because they have no non-operational region. However, as these converters are more complex and are more expensive than Buck or Boost, usually the designers choose the last two. In order to check the Buck and Boost limitations, these two converters must be studied more deeply. In sequence, some simulations results of the buck converter will also be presented.

ALGORITHM FOR FINDING MAXIMUM POWER POINT

The MPPT controller is a power electronic DC/DC chopper or DC/AC inverter system inserted between the PV array and its electric load to achieve the optimum characteristic matching, so that PV array is able to deliver maximum available power which is also necessary to maximize the photovoltaic energy utilization. PV cell has a single operating point where the values of the current and voltage of the cell result in a maximum power output. These values correspond to a particular resistance, which is equal to *V/I* as specified by Ohm's Law. Also the PV cell has an exponential relationship between current and voltage, so the maximum power point (MPP) occurs at the knee of the curve, where the resistance is equal to the negative of the differential resistance (V/I = -dV/dI).

Additional current drawn from the array results in a rapid drop of cell voltage, thereby reducing the array power output. The aim of this MPPT sub-system is to determine just where that point is, and to regulate current accordingly and thus to allow the converter circuit to extract the maximum power available from a cell. The control methodology presented in this paper will adopt an approach in which designing of the power converter is done by using the relationship existing

between the short-circuit current I_{sc} and the MPP current I_m. By simulating with various sample data for I_{sc} and I_m it is ascertained that the ratio of I_m to I_{sc} remains constant at 0.9. One such control scheme is shown in the figure 8.

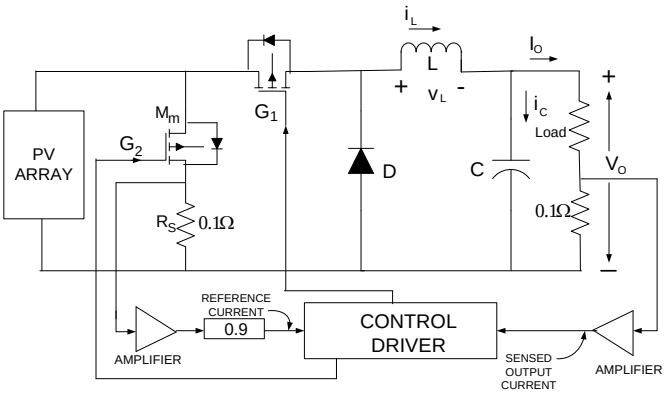

Fig. 11 - MPPT Implementation on a PV array

Determining the MPP for a specific insolation condition and operating the converter for this condition is the critical part in the design of PV conversion system. Initially the short circuit current I_{sc} is measured and then the actual load current adjusted in such a way it is equal to a desired fraction value of $0.9I_{sc}$.

CHAPTER 5

BUCK CONVERTER

A buck converter falls in to the category of switch-mode DC-DC converters. These switch-mode DC-DC converters convert one DC voltage level to another level by temporarily storing the input energy and then releasing that energy to the output at a different voltage level. The preferred storage element can be either a magnetic field storage component (inductors) or electric field storage components (capacitors). This conversion methodology has greater power efficiency (often 75 to 98 percent) than linear voltage regulation (which dissipates unwanted power as heat). A buck-converter produces a lower average output voltage than the DC input voltage V_{dc}. Regulated DC power supplies and DC motor speed control are the main applications.

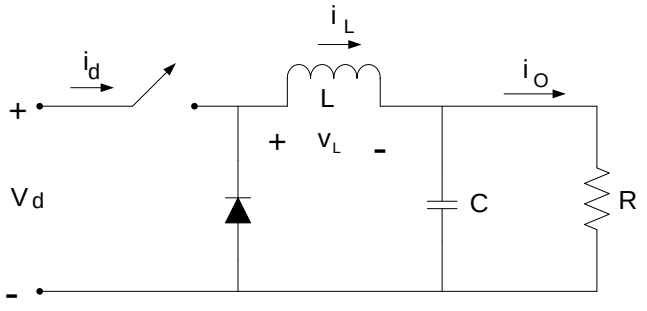

Fig. 12 – Buck Converter Topology

Figure 12 shows the topology of the Buck converter.

$$V_o = \frac{1}{T_s}\int_0^{T_s} V_o(t)dt = \frac{1}{T_s}\left(\int_0^{t_{on}} V_d\, dt + \int_{t_{on}}^{T_s} 0\, dt\right) = \frac{t_{on}}{T_s}V_d = DV_d \qquad (5.1)$$

When an ideal condition is assumed i.e. an ideal switch, a constant input voltage V_{dc} and a pure resistive load, then the instantaneous voltage waveform is shown in figure 13 as a function of the switch of position. Generally the average output voltage is expressed in terms of the switch duty ratio.

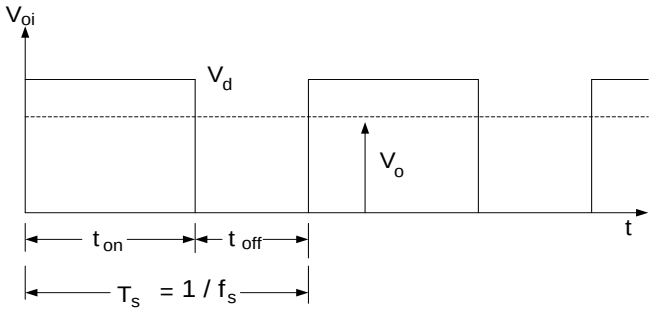

Fig. 13 – Input Voltage as a function of Switch position

It is noted that the diode enters the reverse biased mode during the interval when the switch is ON and the input provides energy to the load as well as to the inductor. During the interval when the switch is OFF, the diode carries the inductor current flowing in the circuit and transfers some of stored energy of the inductor to the load. Under the ideal conditions the filter capacitor at the output is assumed to be very large. This is the common consideration in applications requiring a constant or nearly constant instantaneous output voltage $v_o(t) \cong V_o$. Figure 14 shows the average inductor current in the buck-converter which is equal to the average output current I_o, the main reason behind this being the average capacitor current in the steady-state is zero.

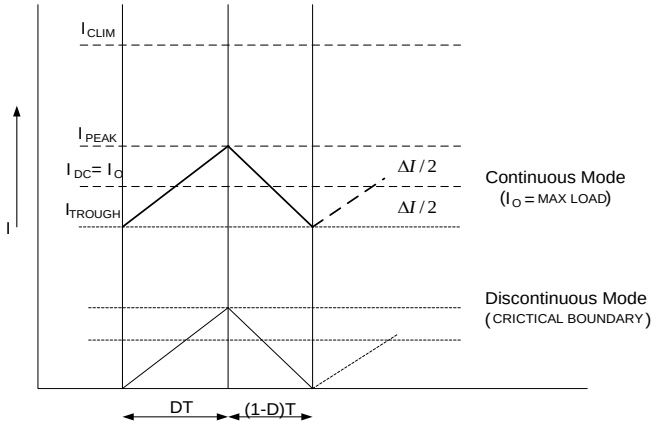

Fig. 14 – Inductor Current

INDUCTOR AND CAPACITOR DESIGN

Inductor voltage current relation is given by $L\frac{di}{dt}$. During time interval T_s, the change in the inductor current Δi_L and voltage across the inductor is $(V_d - V_o)$. Hence, we have

$$\Delta i_L = \frac{(V_d - V_o)DT_s}{L} \tag{5.2}$$

$$I_L = I_o = \frac{V_o}{R} \tag{5.3}$$

which yields a current ripple of

$$\frac{\Delta i_L}{I_L} = \frac{(1-D)RT_S}{L} \tag{5.4}$$

The charge carrying capacity of the capacitor must be (refer fig. 14)

$$\Delta q = \frac{1}{2}\frac{\Delta i_L}{2}\frac{T_S}{2} = \frac{\Delta i_L T_S}{8} \tag{5.5}$$

$$\Delta V_o = \frac{\Delta q}{C} = \frac{\Delta i_L T_s}{8C} = \frac{V_o(1-D)T_S^2}{8LC} \tag{5.6}$$

So, the value of ripple voltage is given by

$$\frac{\Delta V_o}{V_o} = \frac{(1-D)T_S^2}{8LC} \tag{5.7}$$

By fixing the average load current, source voltage, average load voltage, voltage and current ripple, the critical minimum values of the inductor and capacitor can be found out using eq. (5.3) and eq. (5.7). In all our analysis, we assume that the converter operates in the continuous current conduction mode. The inductor designed has EI core with 80 turns.

CONTROL OF BUCK CONVERTER

In response to the changes in the output load and the input line voltages there is always a specified tolerance band (e.g. ± 1% around its nominal value) within which the output voltages of the DC power supplies are regulated. A negative-feedback control system is used to accomplish this as shown in figure 15. Here the output voltage v_o of the converter is compared with a reference value $V_{o,ref}$. The output from the comparator is fed to an error amplifier [11].

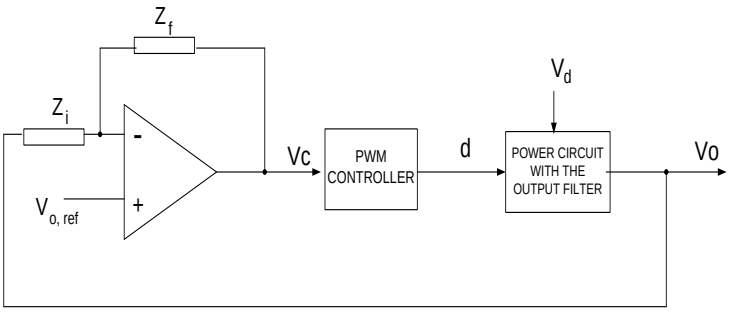

Fig. 15 – Control scheme for Buck Converter

The control voltage v_c is the output from the error amplifier which is used to adjust the duty ratio D of the switches in the converter. With the arrangement of a ramp generator circuit, ramp signal of required frequency is generated. These ramp signals are compared with the control voltage v_c to generate the gate pulses - wherever the control voltage V_e found to be greater than the generated ramp signal a gate pulse is generated.

A proportional controller has been used to accomplish the above mentioned task. It is a linear type feedback control system. The controller output in this proportional control algorithm is proportional to the error signal, which is the difference between the process variable and the set point. In other words, the output of the proportional controller is the product of the proportional gain and the error signal obtained.

ANALYSIS OF BUCK CONVERTER

By analyzing the on-state and off state topologies (fig. 12), we can write the state space model for the system as follows.

ON State:

$$\frac{\mathrm{d}}{\mathrm{dt}}\begin{bmatrix} i_L \\ \mathrm{V}_C \end{bmatrix} = \begin{bmatrix} 0 & \frac{-1}{L} \\ \frac{1}{C} & \frac{-1}{RC} \end{bmatrix}\begin{bmatrix} i_L \\ V_C \end{bmatrix} + \begin{bmatrix} \frac{1}{L} & 0 \\ 0 & \frac{-1}{C} \end{bmatrix}\begin{bmatrix} V_g \\ i_{load} \end{bmatrix} \tag{5.8}$$

$$V_O = [0 \quad 1]\begin{bmatrix} i_L \\ V_C \end{bmatrix} + [0 \quad 0]\begin{bmatrix} V_g \\ i_{load} \end{bmatrix} \tag{5.9}$$

OFF State:

$$\frac{\mathrm{d}}{\mathrm{dt}}\begin{bmatrix}\mathrm{i_L}\\ \mathrm{v_c}\end{bmatrix} = \begin{bmatrix}0 & \frac{-1}{L}\\ \frac{1}{C} & \frac{-1}{RC}\end{bmatrix}\begin{bmatrix}i_L\\ V_C\end{bmatrix} + \begin{bmatrix}0 & 0\\ 0 & \frac{-1}{C}\end{bmatrix}\begin{bmatrix}V_g\\ i_{load}\end{bmatrix} \tag{5.10}$$

$$V_O = [0 \quad 1]\begin{bmatrix}i_L\\ V_C\end{bmatrix} + [0 \quad 0]\begin{bmatrix}V_g\\ i_{load}\end{bmatrix} \tag{5.11}$$

By averaging the two models, we get

$$\dot{x}(t) = [d(t)A_1 + d(t-1)A_2]x(t) + \left[d(t)B_1 + \left(1 - d(t)\right)B_2\right]u(t) \tag{5.12}$$

Linearization of this model is done by incorporating a perturbation to the duty cycle, the state vector and the input voltage. The equation now becomes

$$(\dot{\hat{x}} + \dot{X}) = \left[\left(D + \hat{d}\right)A_1 + \left[1 - \left(D + \hat{d}\right)\right]A_2\right](X + \hat{x}) + [\left(D + \hat{d}\right)B_1 \ + \left[1 - \left(D + \hat{d}\right)\right]B_2](U + \hat{u}) \tag{5.13}$$

Transfering the above equation to Laplace domain, we have

$$\hat{x}(s) = (sI - A_o)^{-1}B_0\hat{u}(s) + (sI - A_o)^{-1}E\hat{d}(s) \tag{5.14}$$

where

$$A_o = DA_1 + (1 - D)A_2 \tag{5.15}$$

$$B_0 = DB_1 + (1 - D)B_2 \tag{5.16}$$

$$E = (A_1 - A_2)X + (B_1 - B_2)U \tag{5.17}$$

From eq. 5.14 we have the transfer function G_{vd} given by

$$G_{vd}(s) = \frac{RV_g}{s^2LCR + sL + R} \tag{5.18}$$

The remaining parts have straight forward transfer functions like K_p for the proportional controller, and $\frac{1}{V_{ramp}}$ for the comparator. Now the system can be analyzed by the classical control theory.

CHAPTER 6

CIRCUIT AND PRACTICAL IMPLEMENTATION

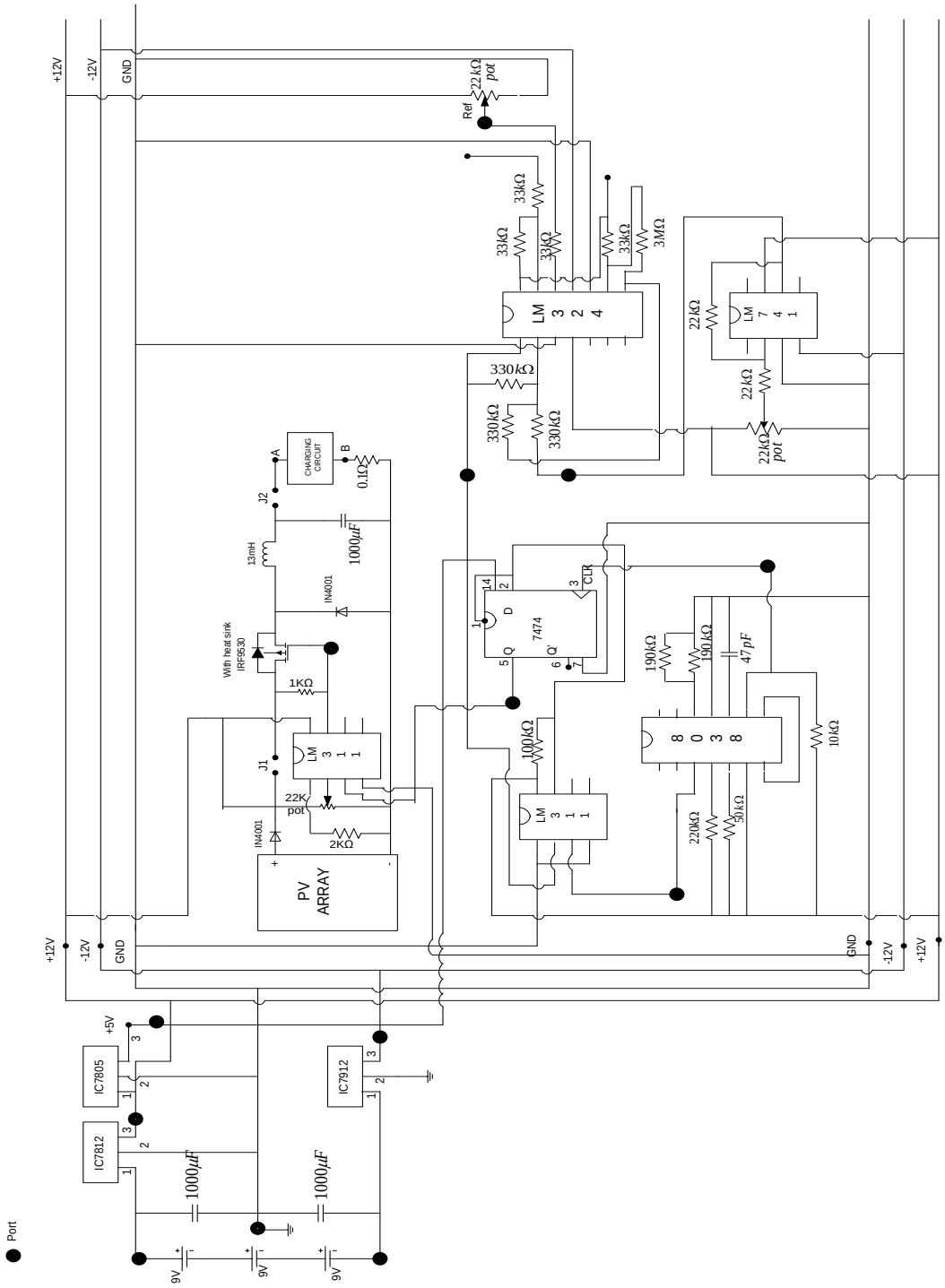

Fig. 16 – The complete circuit of the Buck Converter

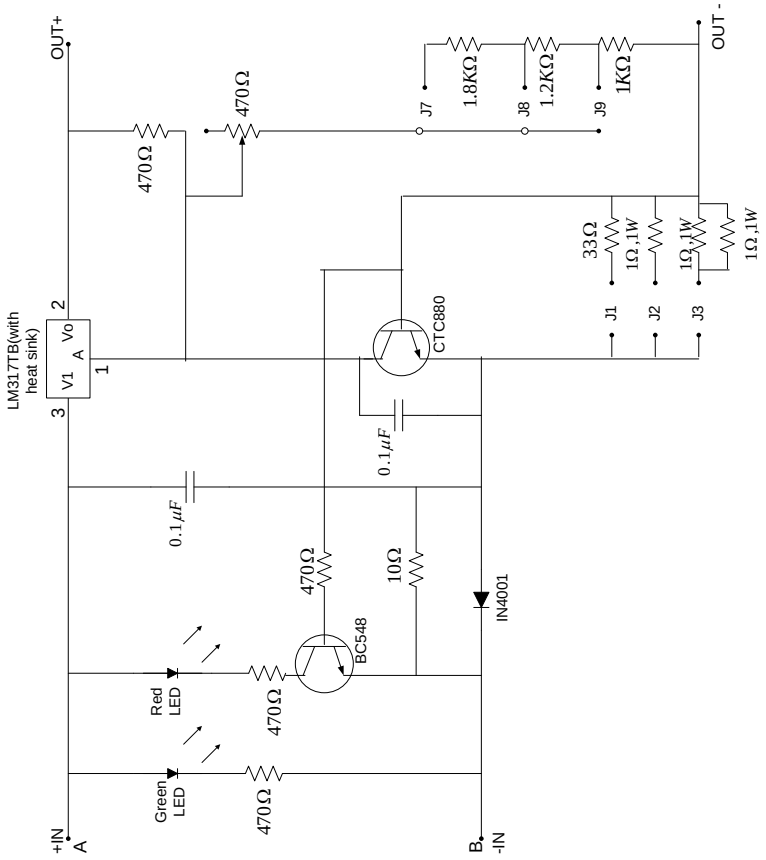

Fig. 17 – Charging Circuit

DESCRIPTION OF POWER SUPPLY

The power supply circuit constitutes the battery, capacitors and voltage regulator ICs required for the voltage regulation. Three 9V batteries are connected in series to give positive and negative terminals for ICs. By using two capacitors of $1000\mu F$ connected in series with a center tapped ground terminal the supply voltage from the three batteries, which is 27V is divided into two 13.5V. There terminal voltage across the positive terminal of the supply along the upper $1000\mu F$ to the center tapped ground terminal is 13.5V. And the between the negative terminal of the supply along the lower $1000\mu F$ capacitor to the center tapped ground terminal produces a voltage of -13.5V. These two supply voltages are the base voltages.

Now with these available supply voltages other required supply voltages are derived with use of different ICs. Starting with the IC 7812, which is basically a linear voltage regulator. The supply voltage of +13.5V is connected to the PIN1 and the PIN2 is grounded. Output from this IC is from PIN3, it produces a +12V. This +12V is connected to the PIN1 of IC 7805 with its PIN2 grounded through the center tapped ground terminal used in the capacitor arrangement. Output of this IC is taken from the PIN3 which produces +5V. This +5V supply is mainly used to supply the flip-flop.

Now in order to derive a -12V supply from the base supply voltage IC 7912 is used. The negative supply terminal voltage i.e. -13.5V is fed to the PIN1 of the IC 7912. And the PIN2 is grounded. The output of this IC 7912 is taken from the PIN3. It produces -12V supply voltage which is mainly used for supplying ICs like LM 741 and LM 324.

POWER CIRCUIT

The power circuit consists of the photovoltaic module, the buck – converter, the filter unit and the load.

PV MODULE

It is basically a packaged interconnected assembly of photovoltaic cells. The photovoltaic module consists of the 36 solar cells arranged in series-parallel pattern to produce16.5V. These solar cells are manufactured using mono crystalline silicon materials. The use of silicon in manufacturing the solar cells achieves its highest efficient usage mainly by incorporating the mono-crystalline cells for photovoltaic modules. In manufacturing these photovoltaic modules the encapsulation of the cells are done by using the UV stabilized polymer (EVA) and the protective back cover using Tedler-Polyester-Tedler [12]. The usage of the high transmission toughened glass superstrate and anodized aluminum frame for mounting the panel are mainly targeted for increasing the service life of these photovoltaic modules. The maximum power rating of this photovoltaic module is 24W. And the current rating is 1.82A. Under nominal operating cell temperature the rated irradiance level is 800W per sq.m. With this whole arrangement within the internal structure is as described above and this photovoltaic module weighs 4.2kg.

MOSFET

The buck-converter consists of a power electronic switch, an inductor, a diode and a capacitor. The power electronic switch chosen is the MOSFET IRF9530NS. It provides the highest power capability with lowest possible on-state resistance, so it is extremely efficient and reliable. With the low internal connection resistance it can dissipate up to 2W. The MOSFET is used with a heat sink.

INDUCTOR

The inductor used has inductance value of 13mH. The inductance value chosen also reflects the static power losses that can occur in this buck-converter circuit. The static power losses constitute the I^2R (conduction) losses in the wires or PCB traces as well as the inductor. The efficiency depends on the conduction losses and the switching losses. But the conduction losses depend on the load and the inductor winding resistance. So the overall efficiency dependent factors include the chosen inductance value. It has a maximum operating frequency of $1MHz$.

DIODE

The diode used is IN4007. These diodes can operate under low forward voltage condition. It has a high current capability with low leakage current and high surge capability. Its operating voltage range is 50 to 100V with an operating current of 1A. The main use of the diode in the buck-converter circuit is to provide a current carrying path during switch OFF mode.

CAPACITOR

The capacitor used has a value of $1000\mu F$. These capacitors used are electrolytic capacitors. With this chosen value of capacitance (i.e. large enough) the terminals are maintained at constant voltage during the commutation cycle. It turn the average value of the current flowing is zero. This output capacitor has enough capacitance to supply power to the load (a simple resistance) without any noticeable variation in its voltage.

The operation of the buck converter is already explained in the Chapter 5.

CONTROL CIRCUIT

The control scheme used is the voltage mode control [13]. Initially a reference voltage signal is generated to create reference voltage which is necessary for the control technique adopted. A voltage divider arrangement is used for generating the reference voltage signal. The potential divider creates the reference voltage which is connected in between +12V and ground. A 22K pot is used for this purpose.

This reference voltage signal generated is compared with the output voltage from the buck-converter. For accomplishing this task IC LM324 is used. It is a single supply quad Op-Amp IC [14]. This quad amplifier can operate at supply voltages ranging from 3V to32V.

OP-AMPS

As shown in the figure 18 the reference voltage signal is connected to the PIN-12 of LM 324 with a 33K resistance in series. PIN-12 is the non-inverting terminal. The output voltage from the buck-converter is connected to the PIN-13, which is the inverting terminal. A 33K resistance is connected in series with the output voltage fed to the LM324. The output for this Op-Amp is taken from the PIN-14. This output voltage is the required error voltage signal, which is connected in series with a 33K resistance to provide a negative-feedback to this Op-Amp. This Op-Amp acts as a differential amplifier.

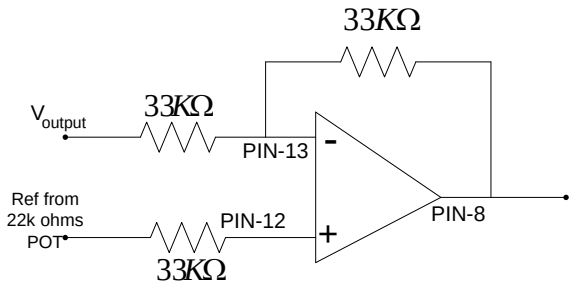

Fig. 18 – Op-Amp used as a differential Amplifier

$$V_{out} = A_d(V_{in}^{+} - V_{in}^{-}) + A_C(V_{in}^{+} + V_{in}^{-}) \quad (6.1)$$

Refer to figure 19. The error voltage signal generated is fed to PIN-9, which the inverting terminal of another Op-Amp in the same chip of IC LM324. A 33KΩ resistance is connected in series with this input error voltage signal. And the PIN-10 is connected to ground as shown in the Figure. The output for this Op-Amp is taken from the PIN-8, which is connected to a 3MΩ resistor as a negative-feedback to the inverting terminal of this Op-Amp. This Op-Amp acts as an inverting amplifier.

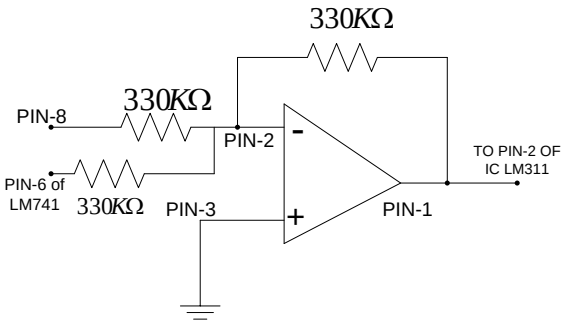

Fig. 19 – LM 324 used as an Adder

The output signal obtained from the PIN-8 is connected to the PIN-2 through a 330KΩ series resistance. PIN-2 is the inverting terminal of another OP-Amp of LM324 (fig. 19). PIN-3, which is the non-inverting terminal of this Op-Amp, is connected to ground terminal. The output of this Op-Amp is taken from the PIN-1, which is connected to a 330KΩ resistance to act as a negative-feedback to this Op-Amp. This Op-Amp can act as an adder.

PIN-2 of LM741 (which is the inverting terminal) is connected to a 22KΩ resistor is which connected to the +12V through a series connected POT of 22KΩ .Simultaneously this point i.e. the terminal from 22KΩ pot connected to the +12V supply. The PIN-3 is the non-inverting terminal of this Op-Amp, this is connected to the ground terminal. The PIN-4 is connected to negative supply of -12V. Refer figure 20.

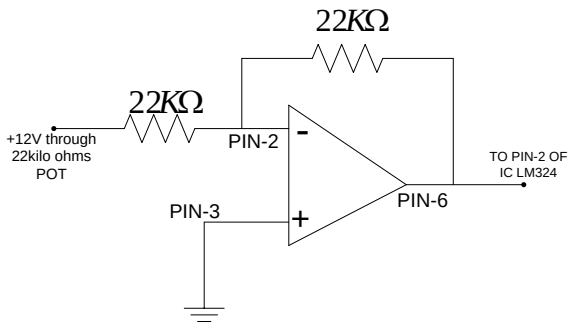

Fig. 20 – LM 741 as an inverting amplifier

The output of this Op-Amp is taken from PIN-6 as shown in the figure; this terminal is connected to the PIN-2 through a 22KΩ resistance in series which acts a negative-feedback to this OP-Amp. This output at PIN-6 is connected to the PIN-2 of the IC LM324. This IC provides a positive or a negative offset. This offset can be added or subtracted respectively by connecting it to PIN-2 of IC LM324.

RAMP GENERATOR 8038

IC 8038 is the ramp generator. This waveform generator is a monolithic integrated circuit capable of producing high accuracy triangular, saw-tooth and pulse waveforms with minimum of external components [15]. In this PIN-4 and PIN-5 are connected to the +12V supply voltage through 220KΩ and 50KΩ series resistor respectively. These are resistors connected at the terminals PIN-4 and PIN-5 are the resistances which decide the rise time and fall time of the ramp signal. The square wave generated by 8038 is tapped at PIN-9 and fed to the clock PIN-3 of IC 7474 (D-Flip Flop).

LM311

LM311 ICs can operate over a wider range of supply voltages i.e. from the standard ±15V op-amp supplies to single 5V supply for IC logic [16]. In these ICs both the inputs and the outputs can be isolated from the system ground and the output can drive loads referred to ground, positive supply or the negative supply.

The output ramp signal generated at PIN-3 of IC 8038 is connected to PIN-3 of IC LM311. PIN-3 of LM311 is the inverting terminal. The output error voltage obtained from the PIN-1 of IC LM324 is connected to the PIN-2 of IC LM311. This voltage comparator compares the error voltage signal and the generated ramp signal to produce the firing signals. The output for this IC is taken at the PIN-7.

GATE PULSE TO DRIVER

The output signal obtained from PIN-7 of IC LM311 is connected to PIN-2 and PIN-1 of IC 7474. PIN-7 is connected to the ground terminal. The square wave pulse generated at PIN-9 of IC 8038 is connected to the PIN-3, which is the clock input to this D –flip flop. The main use of this IC is to provide the same output previously present it till the next clock pulse is provided to the PIN-3. This is used to supply the driver chip of the MOSFET IRF9530NS. The output of this IC is taken at PIN-5.

DRIVER CIRCUIT

The output signal obtained from PIN-5 of IC 7474 is connected to the PIN-3 (which is the inverting terminal) of IC LM311 (which acts as the driver chip of MOSFET IRF9530NS). PIN-1 is connected to the negative supply terminal of the Photovoltaic module through a 2KΩ series resistance. PIN-4 is connected to the ground terminal. +12V supply voltage is connected to PIN-2 (which is the non-inverting terminal) through a 22KΩ POT. PIN-8 is connected to the +12V supply voltage terminal. The output for this IC is taken at PIN-7 i.e. the gate pulses are generated at this PIN. This output signal is connected to the gate of MOSFET IRF9530NS.

CHARGING CIRCUIT

The charging circuit is connected across the output load terminal of the buck-converter circuit. The green LED indicates the supply voltage. A 470Ω resistance is connected in series to protect the LED. Another set consisting of a red LED and a 470Ω resistor connected in series with a transistor BC548 are connected in parallel to the previous arrangement as shown in the figure 17.

The positive supply terminal is directly connected to the PIN-3 of IC LM317TB.This IC is used as a voltage regulator. This IC can supply more than 1.5A of load current with an adjustable output voltage range of 1.2 to 37V. The variable resistor must be set to give the requires output voltage (approx. 4.5V for charging one cell). PIN-1 of the IC LM317TB is connected the power transistor CTC880. And the load to be charged is connected across the terminals marked as OUT+ and OUT- as shown in the figure.

There are some jumpers available in this charging circuit to facilitate better usage of this circuit. Jumpers J7, J8 and J9 are connected to charge one, two and three cells respectively. Jumpers J1, J2 and J3 decide the charging rate of the batteries. But among all these options generally the jumper j1 is preferred. This type of charging is called the trickle charging. This takes a long duration for charging, but this type of charging is good for the service life of batteries.

When the supply is ON and the battery is charging, transistor CTC880 switches ON the red LED. This will indicate the charging mode of the circuit. So during the charging time both the green and the red LEDs will glow. The red light is off when the battery is fully charged.

CHAPTER 7

RESULTS AND DISCUSSION

SIMULATION RESULTS

The figure below shows the complete block diagram of the circuit. This includes the PV module block, the power circuit and the control circuit. The modeling and the simulation of the whole system has been done in MATLAB – SIMULINK environment.

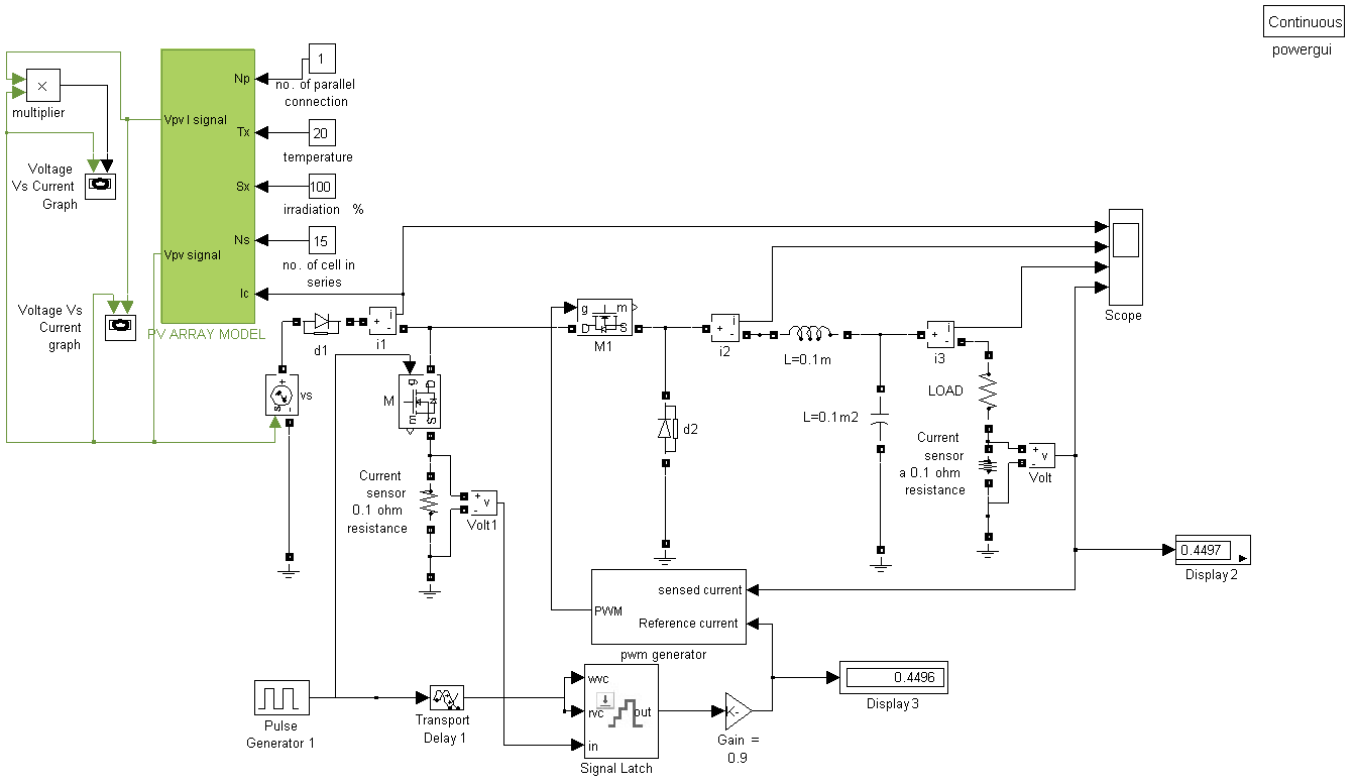

Fig. 21 - Complete simulation model of the photovoltaic energy conversion system

PV SIMULINK MODEL BLOCK

Fig-22 shows the complete PV cell Simulink model block. The various input parameters include photocurrent, reference cell operating temperature, cell output current and solar insolation level. Scope1 will show the response of the cell output voltage.

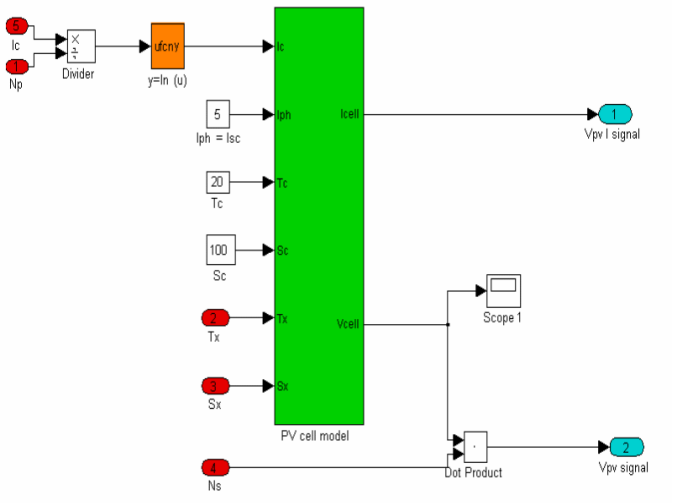

Fig. 22 - Complete PV Cell Simulink model block

INTERNAL COMPONENTS OF PV SIMULINK MODEL

Fig-23 shows the block diagram of the photovoltaic sub-module used to measure the cell output current and voltage. The radiation and the temperature effects are taken into consideration, which is done using a sub-module shown in the below figure. The input parameters chosen to solve the equation-1 (see eq. 3.1) are cell output current, photocurrent at changed condition and the cell operating temperature as shown in fig-23.

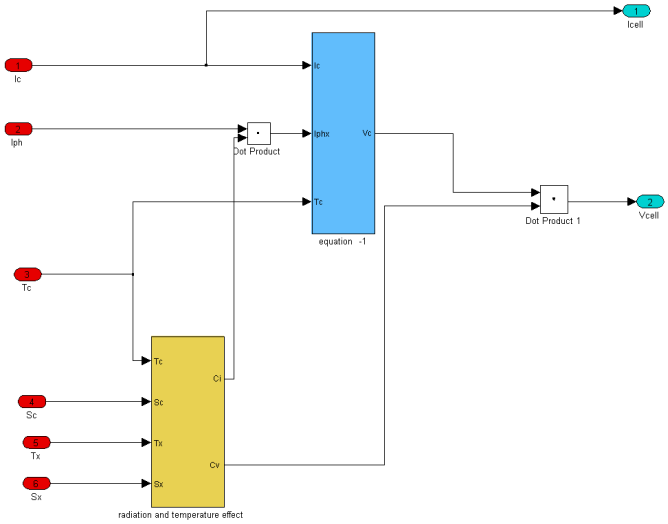

Fig. 23 - Block diagram of the PV sub-module that gives out cell current and cell voltage

Figure 24 shows the block diagram of the photovoltaic sub-module used in determining the correction factors for change in cell current and cell voltage. The input parameters chosen includes the temperature coefficients for cell output voltage and cell photocurrent and the solar insolation level coefficients for cell output voltage and cell current.

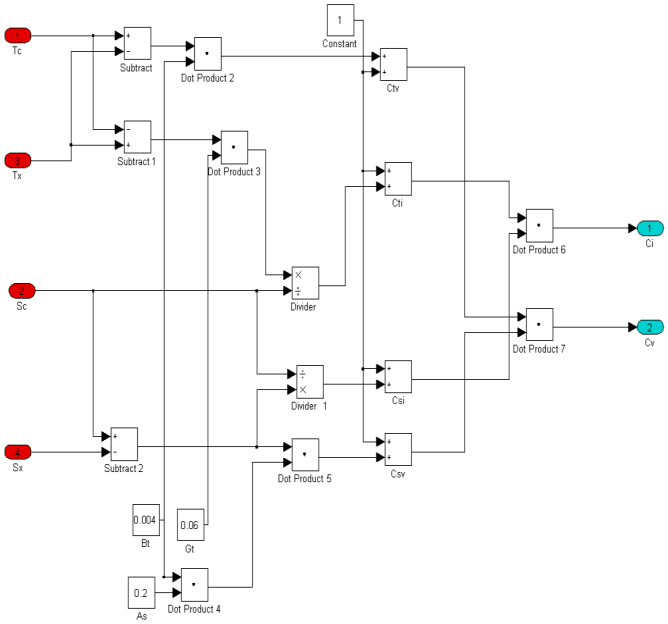

Fig. 24 - Block diagram of PV sub-module that determines correction factors for current

Figure 25 shows the block diagram of the photovoltaic sub-module used in calculating the PV cell output voltage. The input parameters chosen are cell output current, cell photocurrent and the operating temperature of the cell. Some of the input constants are temperature conversion constant, Boltzmann constant, ideality factor and electron charge.

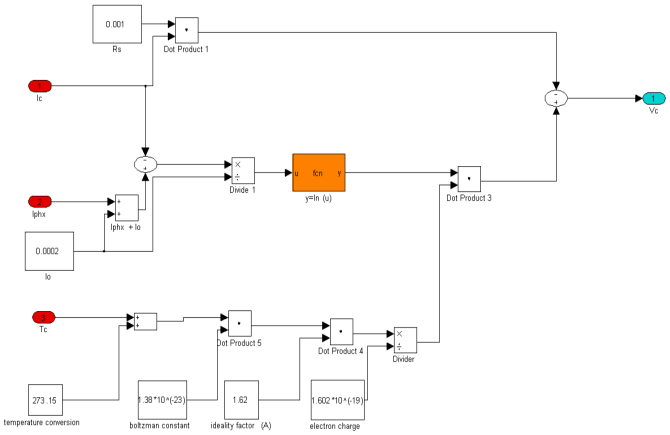

Fig. 25 - Block diagram of PV sub-module that measures PV cell output voltage

Figure 26 shows the block diagram of internal sub-module blocks that constitutes the PWM generator. The proportional gain controller is chosen in this case. Some of the input parameters chosen are reference current and sensed current. Initially these two currents are passed through a subtracter and then multiplied by a gain K(=1000000).

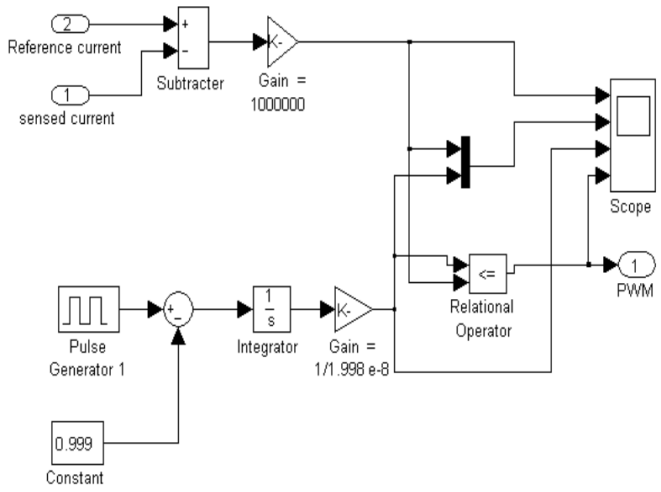

Fig. 26 - Block diagram of the internal sub-modules of PWM generator

OUTPUT WAVEFORMS OF BUCK CONVERTER AND CONTROL CIRCUIT

Fig-27 shows the error voltage signal obtained from the PIN-1 of *IC LM*324. Initially the error signal is high and gradually reduces to a lower value.

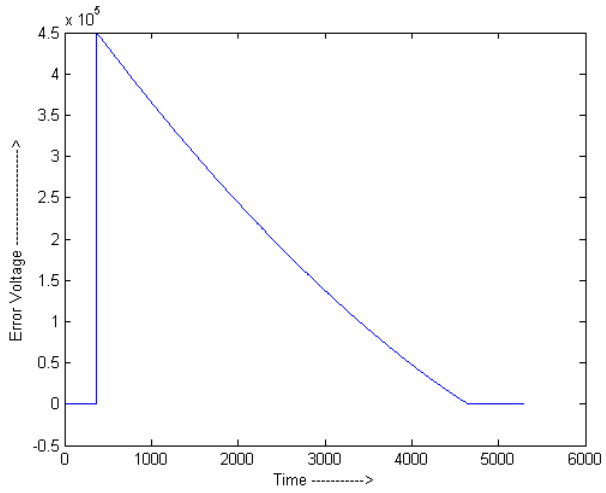

Fig. 27 - Response of the error voltage signal from the comparator

Fig-28 shows the generated ramp voltage signal. This ramp signal is taken from PIN-3 of *IC* 8038. The frequency of the generated ramp signal can be calculated using the following expression.

$$f = \frac{1}{t_1 + t_2} = \frac{1}{\frac{R_A C}{0.66}\left(1 + \frac{R_B}{2R_A - R_B}\right)} \tag{7.1}$$

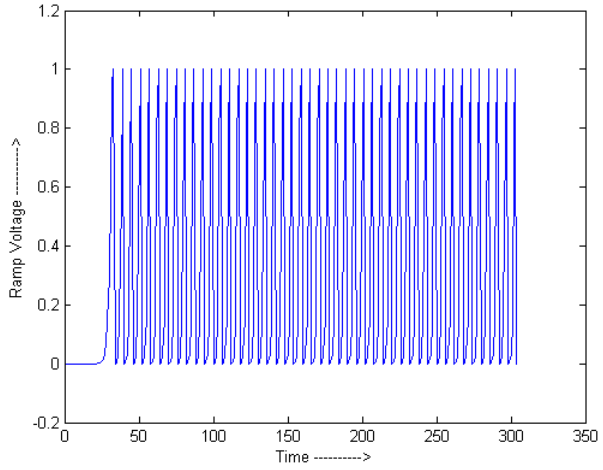

Fig. 28 - Response of the ramp voltage generated

Fig-29 shows the gate pulse generated by comparing the sensed current and the reference current. The thicker band indicates the response during the switching condition.

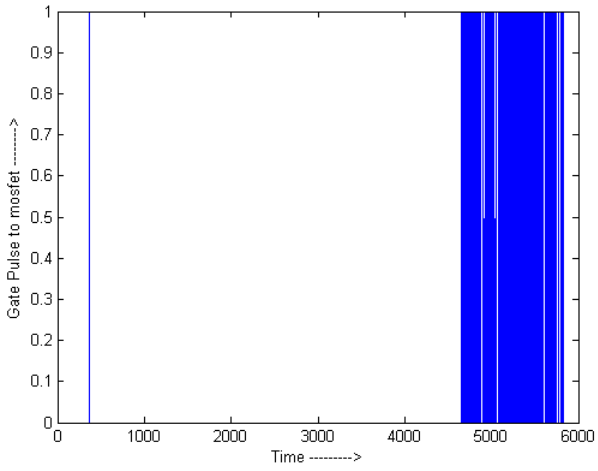

Fig. 29 - Generated gate pulse from the PWM controller

Fig – 30 shows the inductor current waveform. With higher value of inductance the ripple current ratio reduces and with a lower RMS current in the output capacitor can be observed.

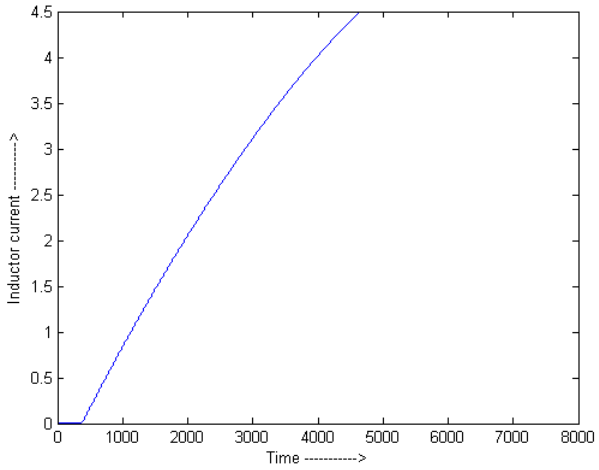

Fig. 30 - Current response of the inductor

Fig - 31 shows the voltage across of the inductor. Initially the voltage remains at zero value. Within a short duration it reaches around 5.2V. Then it gradually decreases under the switched off condition. The thicker band indicates the fluctuations of the voltage across the inductor under switching conditions.

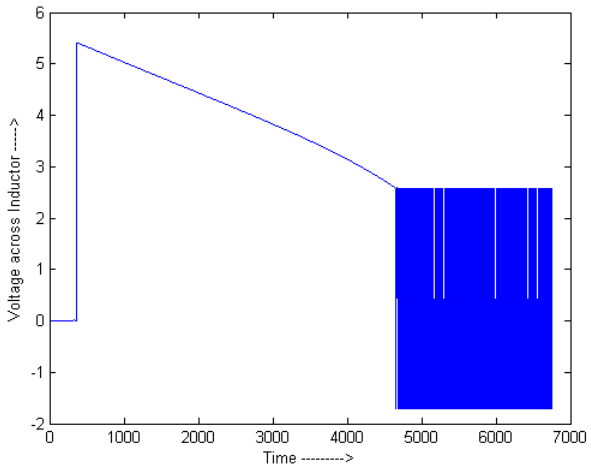

Fig. 31 - Response of the voltage across the inductor

Fig-32 shows the sensed output current, which is sensed at the output of the buck converter circuit. A 0.1Ohm resistor is used for sensing this output current.

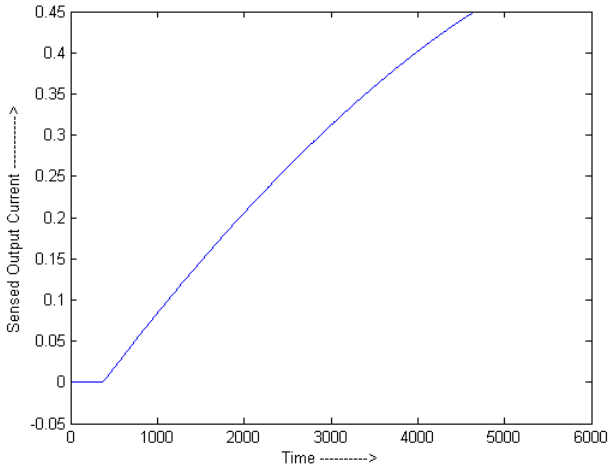

Fig. 32 - Response of the Sensed output current

Fig-33 shows the reference current sensed from the power circuit. This reference current is sensed only once in a duration. Therefore, only one single pulse in the beginning is shown in the above figure.

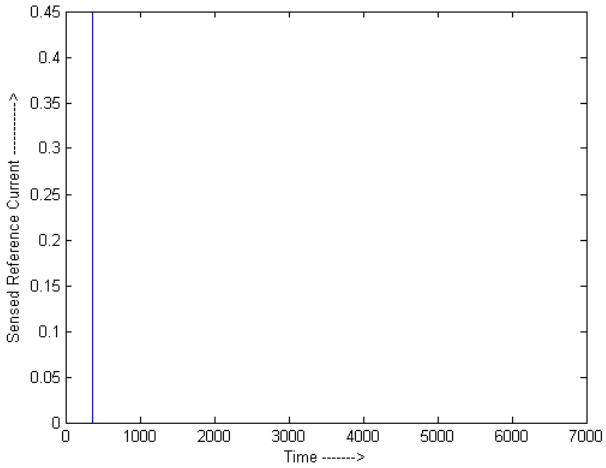

Fig. 33 - Response of the sensed reference current

Fig-34 shows the voltage across the MOSFET IRF9530NS. Initially the curve starts with an offset value of 1V. Then with a steep increase it reaches 5.4V. This occurs under the switched off condition. Under switch ON condition MOSFET acts as a short, so the voltage reaches the zero value as shown in the figure. With the practical case there is always an on-state voltage drop, which is a negligible value. The thicker band indicates the fluctuation of the voltage across the MOSFET during the switching condition.

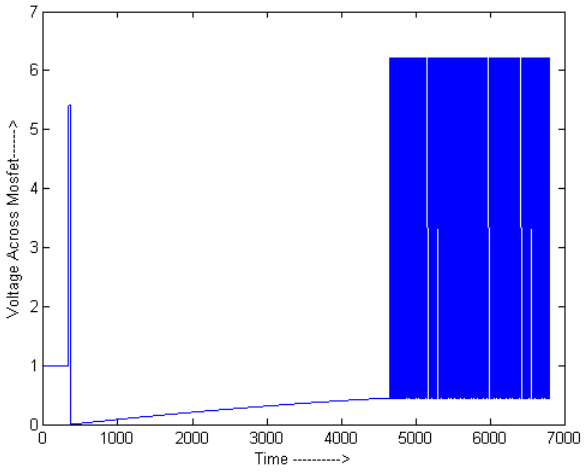

Fig. 34 - Response of voltage across MOSFET IRF9530NS

OUTPUT WAVEFORMS OF PHOTOVOLTAIC ARRAY

Fig-35 shows the output voltage across the supply terminals of the photovoltaic array. Initially the voltage is low, suddenly the value increases to a value around 6.2V. The gradual dip of the curve indicates the voltage variations that occur in a practical circuit. The thicker band indicates the fluctuation of the output voltage under the switching condition. When the current decreases to zero the output voltage is equal to the open circuit voltage and vice versa.

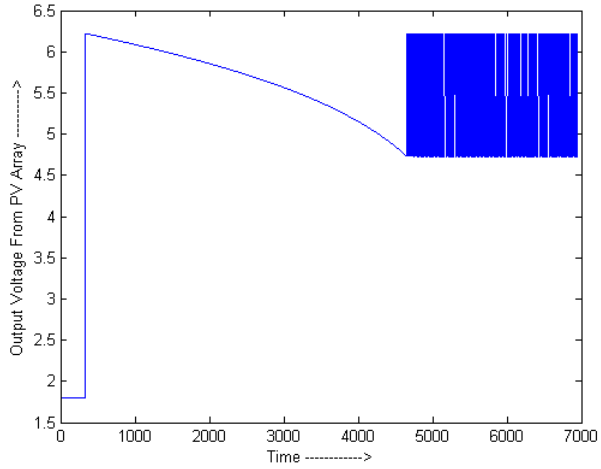

Fig. 35 - Response of the output voltage from the photovoltaic array

Fig-36 shows the output current of the photovoltaic array. Initially the short-circuit current is measured, which is around 5A as shown. Instantly, the current decreases to zero. With the MPPT control technique the current increases gradually to 0.9 times the short-circuit current value. When the current reaches 4.5A it becomes a constant. The thicker band indicates the output current fluctuation during the switching condition.

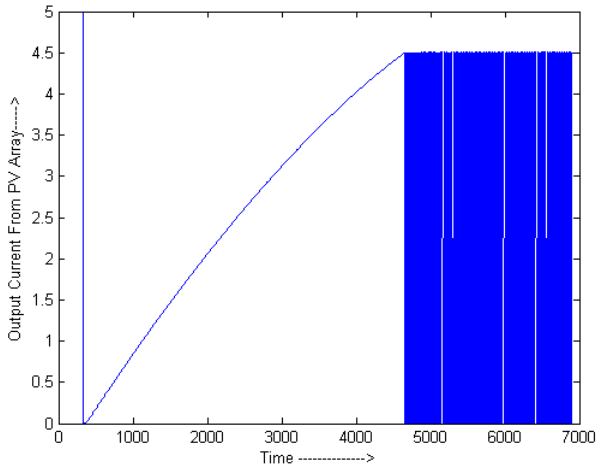

Fig. 36 - Response of the output current of the photovoltaic array

Fig-37 shows the trajectory of the operating point when the reference current is measured. Initially the curve starts with the value equal to the zero current. With the steep increase in the output current value, at short-circuit current value the output voltage is a small finite voltage value from the PV array. Then with adopted MPPT control scheme the current gradually increases to the MPP current.

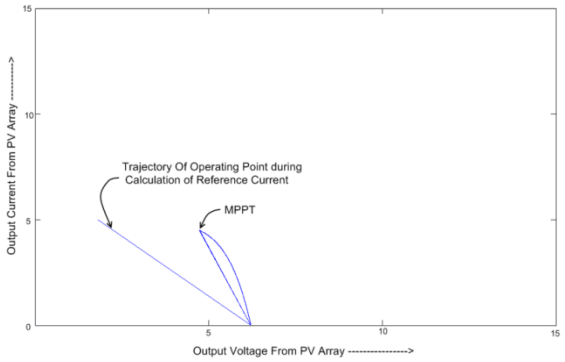

Fig. 37 - Trajectory curve of the operating point in the plot between output current Vs output voltage

Fig-38 shows the trajectory of the operating point when the reference current is calculated. Initially the curve starts at the zero power output value. Then the power increases to nearly 10W, where the initial short-circuit current is measured. With the adopted MPPT control technique the output power increases gradually to the MPPT power value.

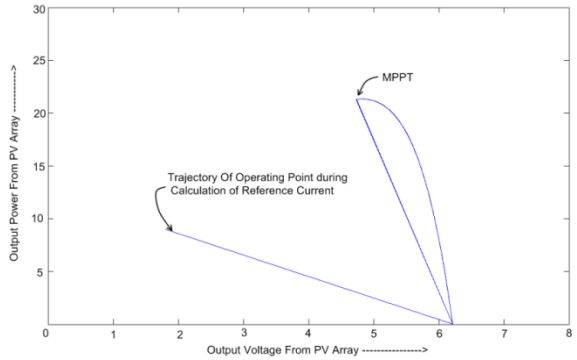

Fig. 38 - Trajectory curve of the operating point in the plot between output power Vs output voltage

HARDWARE OF THE CIRCUIT IMPLEMENTED

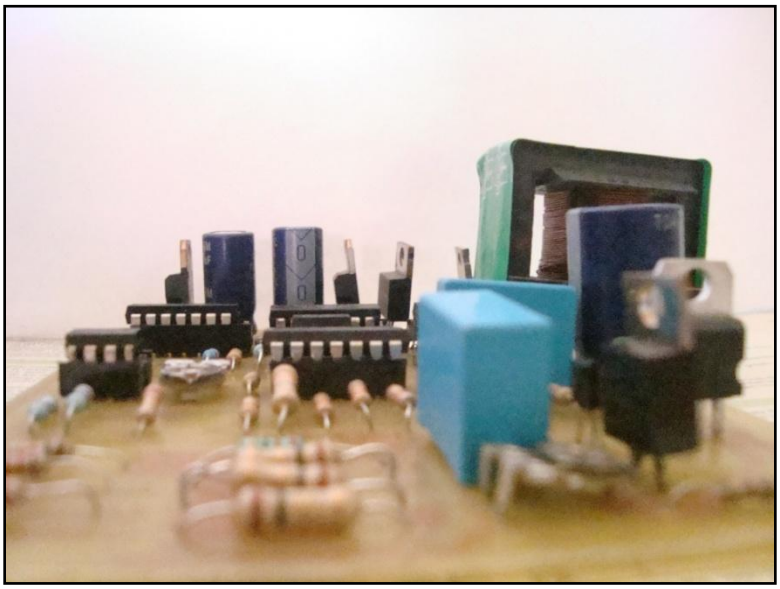

Fig. 39 - Photograph of the PCB designed

Fig. 40 - The complete experimental setup

EXPERIMENTAL RESULTS / WAVEFORMS FROM CRO

The outputs obtained are direct results from the CRO.

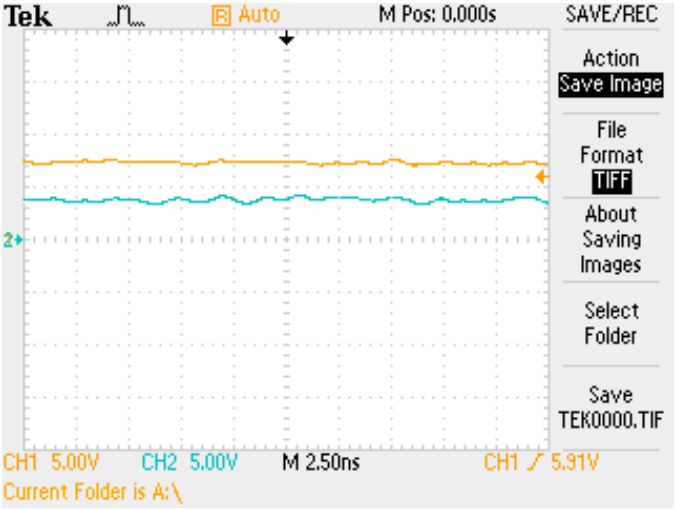

Fig. 41 - Reference voltage (blue) and Output voltage (yellow) in 2.5ns resolution

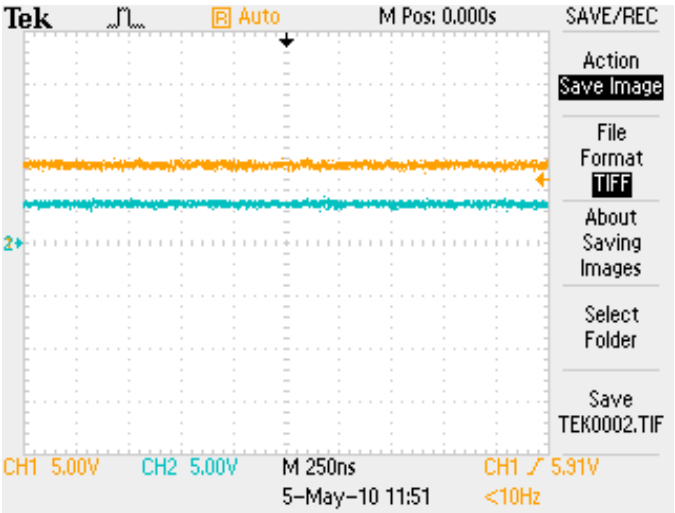

Fig. 42 - Reference voltage (blue) and Output voltage (yellow) in 250ns resolution

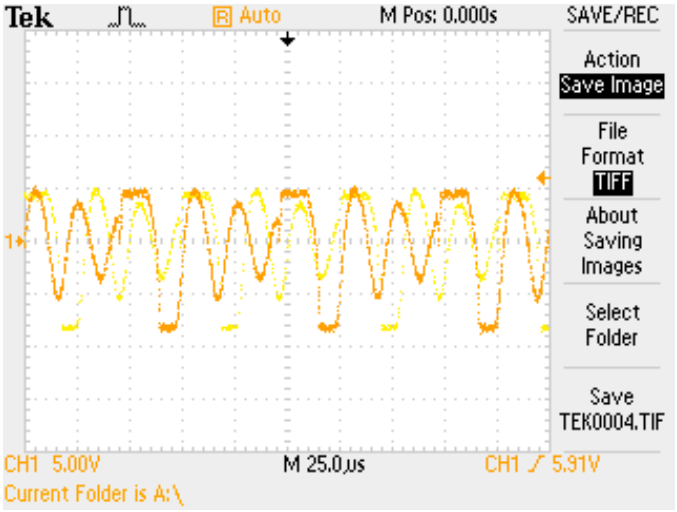

Fig. 43 - Inductor voltage

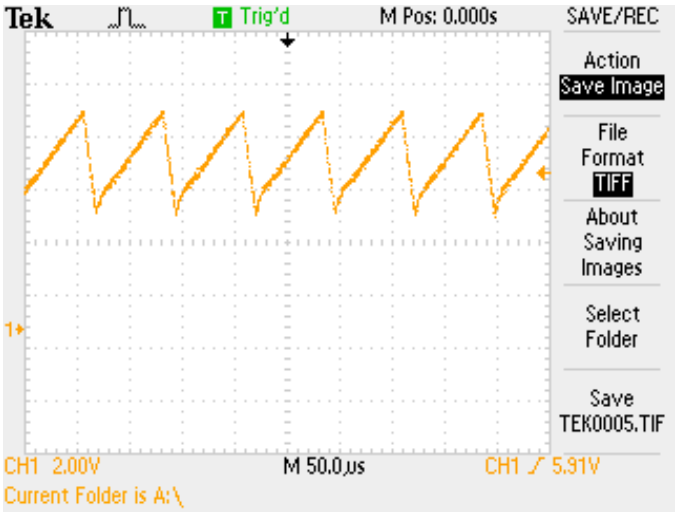

Fig. 44 - Generated Ramp Signal

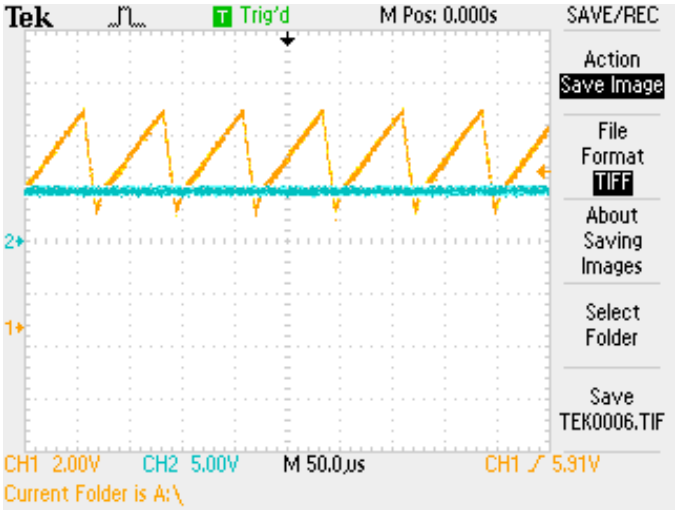

Fig. 45 - Error Signal (blue) and Ramp Signal (yellow)

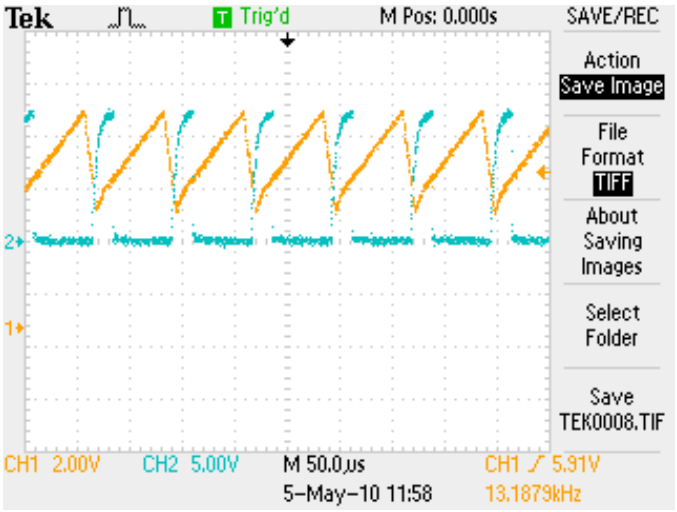

Fig. 46 - Comparator's output (blue) and Ramp signal (yellow)

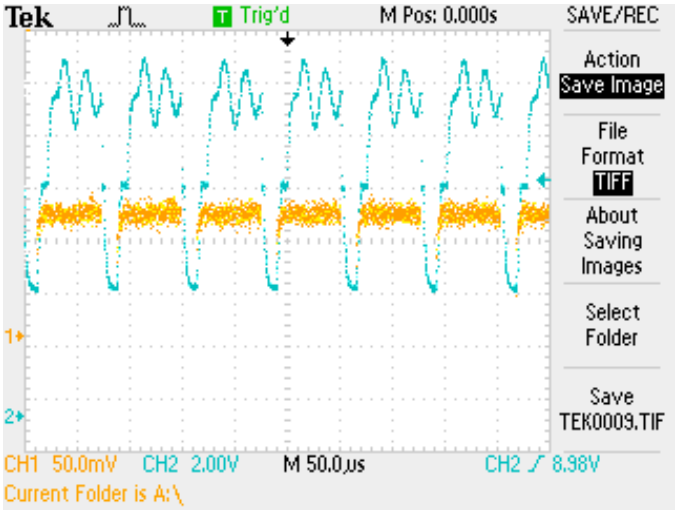

Fig. 47 - Comparator output (yellow) and Gate signal (blue)

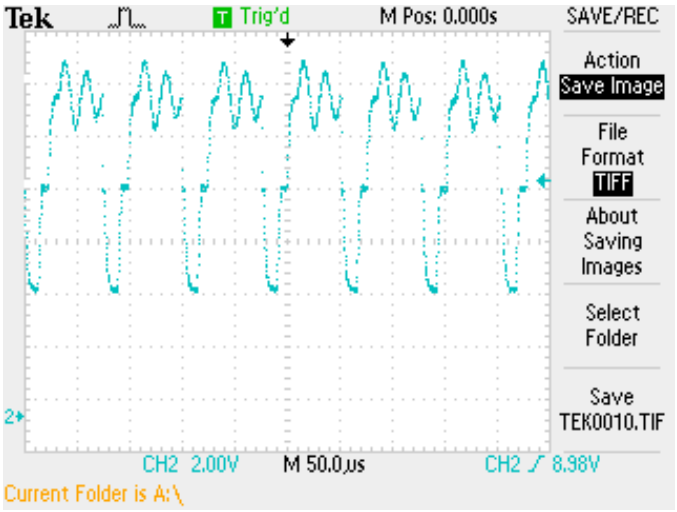

Fig. 48 - Gate signal with respect to ground

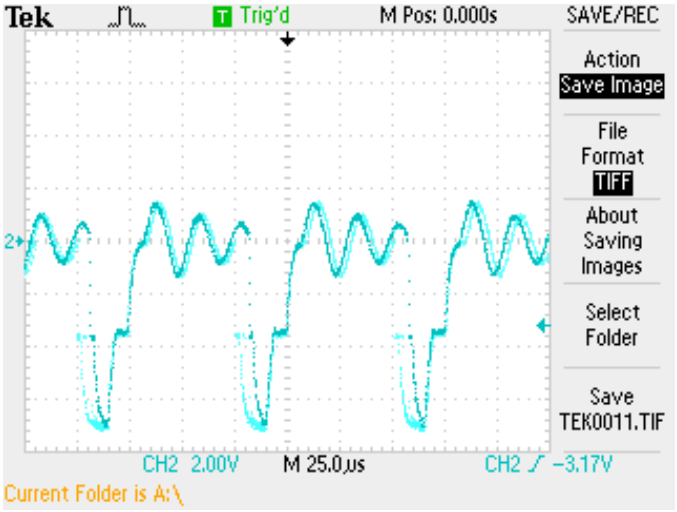

Fig. 49 - Gate signal with respect to Source

CHAPTER 8

CONCLUSION AND FUTURE WORK

From the observations made above, we conclude that the system developed is capable of extracting maximum power from the photovoltaic module at the same time providing a regulated DC supply. The results obtained from experiment are in synchronism with the theoretical results.

The ambient temperature of the system is assumed not to change for a reasonably long time (about 5 minutes). But practically, his may not be the case. The insolation may change in two to three minutes. In such cases, we need to derive the reference voltage from the short circuit current of the PV panel. The value obtained can be latched as the reference voltage and MPP can be obtained automatically without any manual intervention.

REFERENCES

[1] I.H. Atlas and A.M. Sharaf, "A Photovoltaic Array Simulation for Matlab-Simulink GUI Environment", Proce. of *IEEE International Conference on Clean Electrical Power, ICCEP 2007,* Capri, Italy.

[2] Roberto F. Coelho, Filipe Concer, Denizar C. Martins, "A Study of Basic DC-DC Converters Applied in Maximum Power Point Tracking", Proceedings of IEEE 2009 Conference, ISBN : 978-1-4244-3370-4, pp. 673-677.

[3] Resources from Ministry of New and Renewable Energy, Annual Report 2009, http://mnre.gov.in/

[4] Abou El-Maaty Metwally Metwally Aly Abd El-Aal, "Modeling and Simulation of a Photovoltaic Fuel Cell Hybrid System", Dissertation for Dr.-Ing, University of Kassel, Germany, 15 April 2005.

[5] Christian DUMBS, "Development of analysis tools for Photovoltaic hybrid systems", PhD Thesis, Ecoledes Mines de Paris 1999.

[6] J.C. Amphlett, R.M. Baumert, R.F. Mann, B.A. Peppley and P.R. Roberge. "Performance Modelling of the Ballard Mark IV Solid Polymer Electrolyte Fuel Cell: II Emperical model Development", *Journal of the Electrochemical Society*, Vol 142, No. 1, 1995, pp. 9-15.

[7] T. Esram, P.L. Chapman, "Comparison of Photovoltaic Array Maximum Power Point Tracking Techniques", *IEEE Transactions on Energy Conversion*, Vol. 22, N 2, pp. 439-449, June 2007.

[8] Pandey, N. Dasgupta, A.K. Mukherjee, "A Single-Sensor MPPT Solution", *IEEE Transactions on Power Electronics*, Vol 22, N 2, pp-698-700, July, 2007.

[9] S. Yuvarajan, Dachun Yu, Shanguang Xu, "A novel power converter for photovoltaic applications", *Journal of Power Sources*, Elsevier Science, Vol. 135, pp. 327-331, 2004.

[10] D.L. King, J.H. Dudley, W.E. Boyson, "PVSIM: A simulation program for photovoltaic cells, modules and arrays", *Proceedings of the 25th IEEE Photovoltaic Specialists Conference*, May 1996.

[11] Mohan, Uderland and Riobbins, "Power Electronics converters, applications and design", Wiley India, 4th edition 2006.

[12] D.L. King, et al., "Field experience with a new performance characterization procedure for photovoltaic arrays", *Proceedings of the Second World Conference on Photovoltaic Solar Energy Conversion*, July 1998.

[13] Somnath Maity, Tapas K. Bhattacharya, Soumitro Banerjee, "Experimental Study of Chaos and Bifurcation in the Buck Converter", *National Conference on Nonlinear Systems & Dynamics"*, IIT Kharagpur, February 24-26, 2005.

Datasheets

[14] http://pdf1.alldatasheet.com/datasheet-pdf/view/11666/ONSEMI/LM324.html

[15] http://www.intersil.com/data/fn/fn2864.pdf

[16] http://www.national.com/mpf/LM/LM311.html

APPENDIX

List and cost of components used are given below. All components were acquired from the open market. The prices given are approximate.

S. No.	Item name	Quantity	Price in Rs.
1	Diode μr160	1	20
2	P MOSFET IFR9530	1	60
3	Capacitor 47μf	2	10
4	Resistor 0.01Ω	2	14
5	IC 8038	1	450
6	IC 7474	1	18
7	IC LM 324	1	30
8	Capacitor 1000pf	2	16
9	Variable resistor 22K	2	6
10	Pot 47K	2	30
11	IC 7805	1	20
12	IC 7812	1	15
13	Resistance total	One set	40
14	Transistor BC548	1	4
15	Transistor D880	2	60
16	Jumper switch	3	18

17	Led	15	30
18	IC LM 317	2	40
19	Heat sink	1	7
		Total	888

Some components are not included as their price varies a lot with the place of purchase and its value is very less (e.g. connecting wires etc.). The PV array contributes almost 50% of the total cost. Again its exact price depends on the manufacturer. PV module used for this project is manufactured by CEL India. Module model number is PM 648 bearing a serial of 59377.